ANL-ART-138

Evaluation of methods to determine strain ranges for use in SMT design curves

Applied Materials Division

ANL-ART-138

Evaluation of methods to determine strain ranges for use in SMT design curves

Applied Materials Division
Argonne National Laboratory

July 2018

Prepared by

M. C. Messner, Argonne National Laboratory
T.-L. Sham, Argonne National Laboratory
Yanli Wang, Oak Ridge National Laboratory
R. I. Jetter, R. I. Jetter Consulting

Abstract

This report describes progress on developing a new method for creep-fatigue design that reduces over conservatism, improves the treatment of elastic follow up effects, and simplifies the design procedure, when compared to the existing ASME Boiler and Pressure Vessels Code, Section III, Division 5 method for creep-fatigue design. Specifically, this report describes the development of one of the three components of the new creep-fatigue design method: a design analysis method to represent the steady cyclic strain range in a component in elevated temperature service. The method developed here uses an elastic perfectly plastic (EPP) analysis with a pseudoyield stress selected to bound the width of the steady state stress-strain hysteresis loop. The report also provides a description of the in-development creep-fatigue design method, including a plan to complete the method by developing design curves and a method to account for stress multiaxiality.

Table of Contents

List of Figures

List of Tables

1 Introduction

1.1 Motivation and objectives for a new creep-fatigue design method

Section III, Division 5 of the ASME Boiler and Pressure Vessel Code [3] includes two creep-fatigue design methods, one based on elastic analysis and one based on inelastic analysis. A nuclear Code Case allows a third method, based on elastic perfectly plastic (EPP) analysis [2]. All three of these design approaches rely on the same fundamental method for calculating creep-fatigue damage. The method requires computing separate creep and fatigue damages and then uses a damage interaction diagram (D-diagram) to assess the interaction of creep and fatigue.

This approach is very empirical, relying on correlating structural loading conditions to creep, fatigue, and creep-fatigue experiments. The step-by-step procedure is:

1. Calculate a representative strain range in the structure using one of the three types of analysis. Use this strain range and a design fatigue curve, developed from experimental data modified by safety factors, to compute fatigue damage as N/N_f where N is the number of design cycles and N_f is the number of allowable cycles from the design fatigue curve. For multiple cycles sum damage using a linear damage summation rule (i.e. Miner's Rule).

2. Calculate creep damage by constructing a representative stress relaxation history using results from one of the three types of analysis. The Code defines creep damage as $D_c = \int dt/t_r$ where t_r is the time to rupture at a given stress, calculated using a design rupture life correlation generated by lower-bounding experimental data. For multiple cycles sum damage using a linear damage summation rule.

3. Given the separate values of creep damage D_c and fatigue damage D_f consult the design D-diagram to determine whether the point (D_f, D_c) falls inside or outside a design envelope.

There are several aspects of this procedure that may lead to non-optimal creep-fatigue designs:

1. The factors applied to experimental data to generate the design fatigue curve — a factor of 2 on the strain range and 20 on the number of cycles to failure — may be significantly over conservative.

2. The method for computing creep damage is highly empirical and there is limited available experimental data to support it.

3. The three existing analysis methods only approximately account for the effect of elastic follow up on creep-fatigue life. Elastic follow up is described in greater detail below. It tends to reduce the creep-fatigue life of test specimens, all other conditions being equal, and so has a significant effect on the creep-fatigue design of actual components.

4. The D-diagram approach for representing creep-fatigue interaction is over conservative even when compared to the creep-fatigue experimental data used to construct the design envelope.

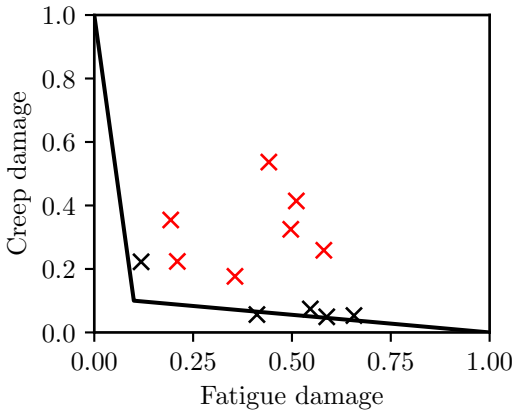

Figure 1.1: Damage diagram and creep-fatigue data from the in-progress ASME Alloy 617 Code Case. The inverse design problem — determine the best-estimate design life for a particular experiment — would provide extremely conservative predicted creep-fatigue lives for the experiments colored in red.

5. The overall procedure has been perceived as complicated and difficult to execute. In general, calculating creep damage with the Code procedure can be challenging, particularly for the elastic analysis methods where the relaxation profile must be constructed through a complicated series of rules designed to account for plasticity and creep in an otherwise linear elastic solution.

Figure 1.1 shows an example of the fourth issue in this list. This figure shows the Alloy 617 D-diagram proposed by an in-progress Code Case and the underlying creep-fatigue experimental data used to justify it. The proposed D-diagram adequately envelopes the available experimental data. However, when compared to the points highlighted in red, it is extremely conservative compared to the data. An improved procedure might reduce this over conservatism.

Most of these issues tends to bias the Division 5 creep-fatigue design procedure towards being over conservative. The Code procedures are viewed by the design community as very conservative, possibly to the point of forcing uneconomical designs.

While all the listed issues are significant this report only addresses the final three. This report describes progress towards an improved creep-fatigue design method that reduces over conservatism, accounts for elastic follow up more accurately, and is easier to execute.

1.2 Description of tentative design method

The design method outlined here is based on experimental data from Simplified Model Test (SMT) specimens. These specimens can be called “key-feature” tests as they represent many of the important aspects of creep-fatigue in actual structural components. Test variables that can be controlled in the SMT framework include the standard creep-fatigue variables of strain range and hold time, but also the elastic follow up factor and the stress concentration factor. Previous publications describe the development of these test specimens [10–12].

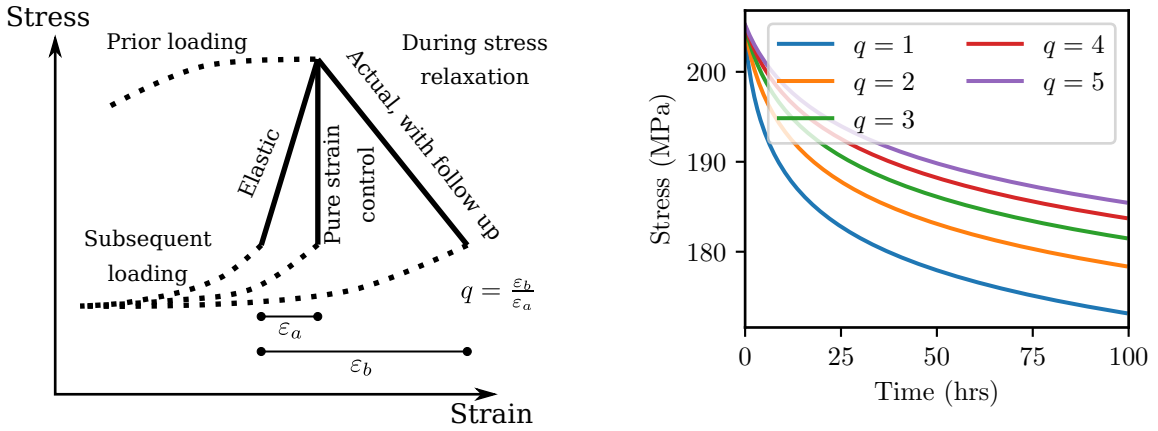

(a) Definition of the follow up factor q.

(b) Effect of follow up on simulated stress relaxation curves.

Figure 1.2: Defining the follow up factor q.

Elastic follow up is resistance to stress relaxation in a test article or component caused by a connection to another structure with a large amount of stored elastic energy. In the uniaxial sense, it is a reduction in the relaxation rate caused by the gauge section being mechanically linked to an elastic spring.

Figure 1.2a shows the definition of the elastic follow up factor, used here to quantify the amount of follow up for a given combination of structural geometry and loading. Note $q = 1$ means follow up has no effect — the loading is purely strain controlled. Figure 1.2b shows simulation results quantifying the effect of follow up on stress relaxation. Increasing amounts of follow up slow relaxation and therefore increase creep damage during the stress relaxation part of a creep-fatigue cycle.

Accurately accounting for elastic follow up is therefore important in the creep-fatigue design of components in elevated temperature service. The current Code rules deal with follow up in an ad hoc manner.

An improved creep-fatigue design method could use data from SMT tests to better capture elastic follow up effects. At the same time the design process could be simplified and the amount of over conservatism reduced to produce more economically efficient designs.

The conceptual design method explored in this report has only two steps:

1. Perform a structural analysis that represents or, at least, bounds the stable cyclic strain range at all points in a component under elevated temperature, cyclic load. Calculate a scalar effective strain from this analysis.

2. Compare the effective strain to a design chart that bounds elastic follow up and creep hold time in high temperature nuclear structural components. The design chart will be setup like a standard fatigue chart; given a strain range it provides a number of cycles to failure. Compare the design allowable cycles to the actual number of design cycles to complete the creep-fatigue design.

This report focuses on the first step in the process: determining a bounding strain range

using a simple structural analysis for components under elevated temperature cyclic load. Chapter 2 describes an elastic perfectly-plastic method of analysis for representing the stable cyclic strain range in such structures. This method is distinct from the previous EPP methods for bounding long-term creep rupture, creep-fatigue damage, and ratcheting strain accumulation. Chapter 3 briefly describes progress on developing design curves from SMT data. Finally, Chapter 4 summarizes the conclusions developed here and discusses a path towards completing the full design method.

2 Simplified method for analyzing design strain ranges

2.1 Method

Under cyclic load the stresses and strain rates at all points will eventually become periodic in a structure made of a material with a constitutive response that can be represented with a standard material model [9]. The specific requirement is that the material response follows Drucker's stability postulate. In this cyclic steady state the strain range — the width of the stress/strain hysteresis loop — does not change cycle to cycle, though the center of the loop may shift in the tensile or compressive directions [4]. The goal of this section is to develop a simple analysis method that can represent or bound this stable strain range for a material with a combined elastic, plastic, thermal, and creep constitutive response.

Elastic perfectly plastic (EPP) methods use an EPP analysis to bound the structural response of a more complicated material. These methods typically retain the elastic and thermal properties of the material but bound creep and plasticity using a pseudoyield stress, which is not necessarily the actual material yield stress. The theory behind these types of bounds has been developed over the past 30 years [5–8]. Two Code Cases allow the use of EPP methods for ratcheting strain accumulation [1] and creep-fatigue damage [2] and an in-progress Code Case will provide a method for bounding long-term creep rupture (i.e. primary load design). These existing methods bound, respectively, ratcheting strain, creep-fatigue damage, and creep rupture stress states. Each of the three existing methods uses a different definition of the pseudoyield stress to bound the relevant quantity. This work develops a similar method to bound the steady state strain range.

Consider the steady cyclic stress-strain hysteresis loop shown in Fig. 2.1 for strain-controlled loading with holds on both the tensile and compressive sides of the cycle. The goal of the EPP analysis is to represent the steady strain range $\Delta\varepsilon$. Intuitively, an EPP analysis using a pseudoyield stress equal to the lowest stress reached during the stress relaxation part of the cycle would bound the width of the full hysteresis loop, as shown on the figure. Approximately, ignoring the effect of prior plasticity and creep on subsequent stress relaxation, this relaxed stress is equal to the value of the material's isochronous stress-strain curve at a time equal to the cycle hold time and at the actual accumulated strain.

The actual accumulated strain cannot be determined directly from a simple bounding analysis and a cycle may have multiple, unequal holds. Using the isochronous curve for the *longest* hold during the cycle produces a conservative strain range, as the figure illustrates. Similarly, using a lower value of the pseudoyield stress than the actual relaxed flow stress will produce a conservative bound. Therefore, it is conservative to use a lower value of strain when determining the pseudoyield stress from the isochronous curve. A reasonable value to use is the apparent yield stress of the isochronous curve for a hold time equal to the cycle period. Using the 0.2% offset provides a flow stress representative of inelastic flow, while conservatively not accounting for any material hardening.

Fundamentally, this is the EPP method adopted here to bound the steady strain range. Because of how the ASME Code defines the material yield stress S_y and the Code isochronous curves it is possible that the isochronous curve apparent yield stress may exceed the Code S_y for short hold times. Therefore, the recommended procedure sets the pseudoyield stress to whichever of the two values is smaller.

The analysis procedure is then:

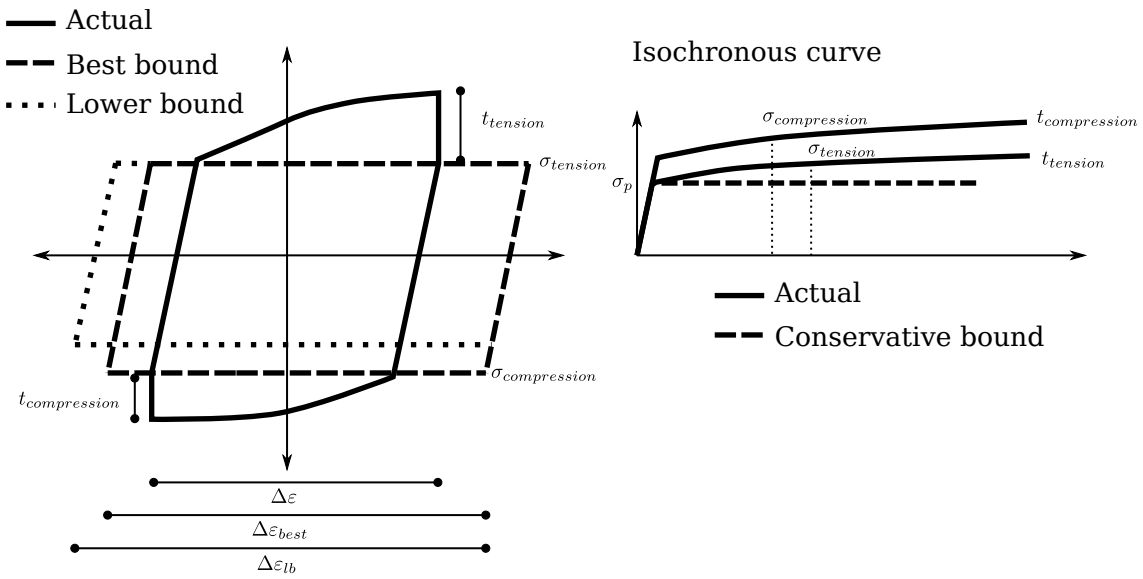

Figure 2.1: Graphical explanation of the EPP methods for bounding steady strain ranges based on material isochronous stress-strain curves.

1. Determine the maximum hold time during the cycle, t_{max}.
2. Determine the pseudoyield stress S_p as the lesser of the material yield stress S_y and the 0.2% offset stress for the material isochronous stress-strain curve for a time equal to t_{max}.
3. Run an analysis of the structure using a EPP material with the actual material elastic and thermal properties and the pseudoyield stress S_p. The analysis can neglect all holds during the loading cycle, as the material model is rate independent.
4. Repeat the load cycle until the structure reaches the cyclic steady state. The analysis does not need to model the full number of design cycles.
5. At each material point determine the steady cyclic strain range $\Delta\varepsilon$ by computing the scalar effective strain from the steady periodic strain components and finding the maximum effective strain range over the steady cycle.

The present report derives the EPP method intuitively, without a formal proof. Future work ought to formalize the method by finding a mathematical bounding theorem. Furthermore, a procedure will need to be created to handle load histories with multiple design cycles, perhaps through a composite cycle approach like the one adopted for the existing EPP Code Cases. Additionally, a scalar effective strain will need to be defined for multiaxial loading. Currently, we use the von Mises strain as a first approximation.

2.2 Validation

The remainder of this chapter validates the EPP method for representing steady cyclic strain ranges. The chapter describes two types of comparisons. The first type is a direct

validation of the model compared to experimental data. The available test data is, at least approximately, uniaxial and includes follow up effects. This means the sample stress state is relatively simple.

The second type of comparison is a consistent comparison to a full inelastic finite element simulation. The idea is to first run a finite element analysis of a potentially complex, realistic component using a reference inelastic model. For this report this reference model is a non-unified model representing 316H stainless steel superimposing an elastic strain, a thermal expansion strain, a rate independent plastic strain, and a rate dependent creep strain. The creep and plasticity models use a standard J_2 flow theory and the plasticity model uses isotropic Voce hardening.

A second finite element simulation is then run to compare to the full inelastic results. This second calculation is an EPP design analysis using consistent design data. In this context, this means the EPP calculation uses the same elastic and thermal properties as the reference model and sets the EPP pseudoyield stress using values of S_y and isochronous curve *determined by simulated experiments using the reference model*. This approach means that the comparison is fair — the full inelastic calculation and the design data are consistent — and means the reference inelastic model does not need to perfectly represent 316H steel, as the design data is consistent with the inelastic model, not the Code design curves. This approach allows the EPP method to be verified for more complicated structures and loading histories than those available from experimental tests.

2.2.1 Comparison to SMT experiments

The first validation test compares the EPP method to SMT experiments conducted at Oak Ridge National Laboratory. These tests were on samples of Alloy 617, and so the design calculation uses the in progress Code Case values of the isochronous stress-strain curves and the material yield stress.

The EPP calculations approximate the SMT geometry with a simple two bar problem. Figure 2.2 shows the assumptions reducing the SMT specimen to two bars in series. The SMT tests applies displacements at the top of the sample, but controls the displacements to apply some cyclic displacement over the inner two stepped regions (δ in the figure). The experimental result is a stress-strain hysteresis loop measured over the inner gauge region (ε in the figure).

The corresponding two bar model assumes symmetry on the specimen centerline and directly imposes the applied displacement to the outer bar 1, rather than control the displacement at that point through feedback control between an extensometer and the machine displacement. The two bar model neglects the triaxial stress state near the transition between the gauge and outer regions.

Oak Ridge National Laboratory has generated a large collection of experiments for Alloy 617 SMT specimens for a variety of imposed displacements δ, with a variety of specific SMT geometries giving different follow up factors q, and at a variety of temperatures T. Additionally, Idaho National Laboratory ran several standard, strain controlled creep-fatigue specimens. Figure 2.3 compares the experimentally-measured steady, average, axial strain range over the inner gauge to the two bar, EPP analysis predictions. In this figure the abscissa plots the EPP strain range from the two bar analysis and the ordinate plots the

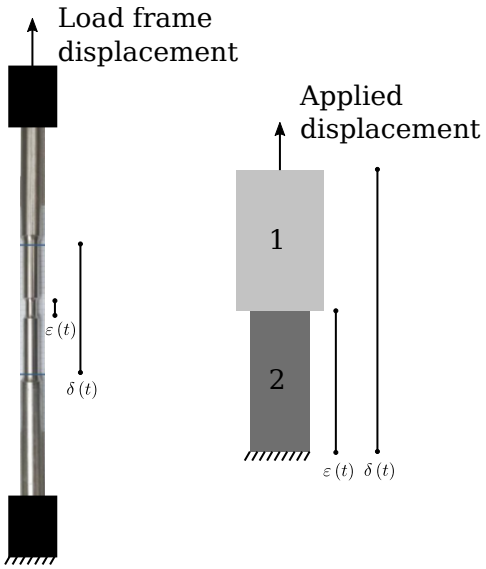

Figure 2.2: Model of the SMT tests as two bar problems.

experimentally-measured strain range. If the analysis method was perfect, that is there was no difference between the experimental and EPP strain range, the data would all fall along the black line plotted on the figure.

The creep-fatigue experiments fall along the line of perfect correlation. This is because these tests are fully-strain controlled — the applied strain range by definition matches the measured strain range — and of the corresponding EPP analysis is likewise fully strain controlled. The more interesting data comes from the SMT tests. In these tests the displacement applied to the outer gauge does not directly relate to the strains in the inner gauge due to plasticity and creep and the geometric difference in cross section between the two sections.

For the SMT data the EPP analysis does not perfectly recover the measured strain ranges. Some error is to be expected as the particular batch of Alloy 617 material will not exactly match the Code description of the material due to heat-to-heat variation, there is some prior history effect neglected by the EPP analysis, and due to general experimental uncertainty. However, the EPP strain ranges strongly correlated with the measured strain ranges, implying that the EPP method can be used to predict realistic design strain ranges for a complete creep-fatigue design method. The squared Pearson correlation coefficient is 0.79, implying a strong correlation between the measured data and the EPP strain ranges. The sample error is approximately uniformly distributed above and below the line of perfect correlation, implying these discrepancies may be due to random error about an average match between the experiments and the approximate design analysis.

2.2.2 Comparison to full inelastic two bar models

The second comparison is a consistent comparison to full inelastic analysis. As described above, the reference inelastic material model approximates the elevated temperature response of 316H stainless steel. Figure 2.4 shows the structural geometry and loading cycle used in

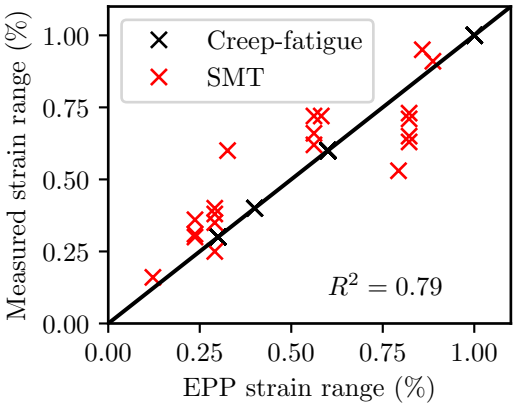

Figure 2.3: Strain range comparison between experimental SMT tests and EPP simulations.

the comparison. The two bars share a constant applied force. The figure shows the cyclic temperature history of each bar. The delay in cooling bar 2 introduces differential thermal expansion into the system, which causes non-uniform creep and plasticity in each of the two bars. The EPP analysis was used to predict the steady cyclic strain range in each of the two bars, compared to the full inelastic analysis, for a variety of loading conditions parameterized by the applied load P and the delay time t_{hold}. The common hold time for both bars at T_{hot} is 1 hour. For these simulations $T_{cold} = 400^\circ$ C, $T_{hot} = 700^\circ$ C, and the heating and cooling rates are both $\dot{T} = 30^\circ$ C/min. Both bars have equal 0.25 in diameters.

Two bar problems are often used to represent vessels under a combination of a primary pressure load and secondary load from a cyclic thermal gradient. As such, this comparison tests to see if the EPP method can accurately represent the steady strain range for a simple realistic structure.

Table 2.1 lists the loading conditions used in the comparisons, the steady strain ranges in each bar for the inelastic and EPP simulations, and the error for each bar between the EPP and full inelastic simulations. In general, the discrepancy between the two calculations is small.

Figure 2.5 is a graphical comparison between the inelastic and EPP simulations. The form of the graph is identical to Fig. 2.3, described above. The graph shows that the EPP and full inelastic strain ranges are nearly perfectly correlated, meaning in the absence of experimental error and with no uncertainty in material properties the EPP method accurately captures the steady strain range in a structural system. Two assumptions of the EPP method, the lower-bounding decision to use the apparent isochronous yield stress and the absence of any prior history effect on the flow stress, cause the small discrepancies between the EPP and the inelastic strain ranges.

2.2.3 Comparison to full inelastic nozzle problem

Figure 2.6 describes the structural geometry and loading for the final validation example. This is another consistent comparison between a full inelastic analysis and the EPP design analysis method. The geometry is an axisymmetric representation of a flat vessel head with

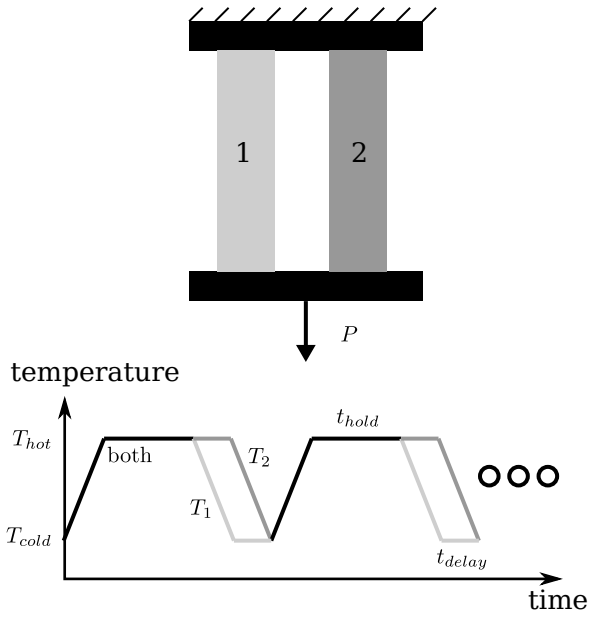

Figure 2.4: Problem setup for the two bar comparison.

P (lbs)	t_{delay} (min)	Inelastic range, bar 1 (%)	EPP range, bar 1 (%)	EPP error, bar 1 (%)	Inelastic range, bar 2 (%)	EPP range, bar 2 (%)	EPP error, bar 2 (%)
50	10	0.25	0.24	4.0	0.29	0.28	3.5
150	10	0.25	0.24	4.0	0.29	0.28	3.5
300	10	0.25	0.25	0.0	0.29	0.29	0.0
450	10	0.25	0.3	-20.0	0.29	0.27	6.9
-100	5	0.15	0.15	0.0	0.16	0.16	0.0
-100	10	0.25	0.26	4.0	0.31	0.31	0.0
-250	3	0.09	0.09	0.0	0.1	0.1	0.0
550	3	0.09	0.09	0.0	0.1	0.1	0.0
-550	3	0.09	0.09	0.0	0.1	0.1	0.0
-250	5	0.15	0.15	0.0	0.17	0.16	0.0
-100	8	0.23	0.25	-8.7	0.28	0.3	5.9
450	7	0.21	0.21	0.0	0.23	0.22	-7.1
-550	5	0.15	0.15	0.0	0.17	0.16	5.9
450	5	0.15	0.15	0.0	0.16	0.16	0.0

Table 2.1: Comparison between full inelastic analysis and simplified EPP analysis for the two bar problem.

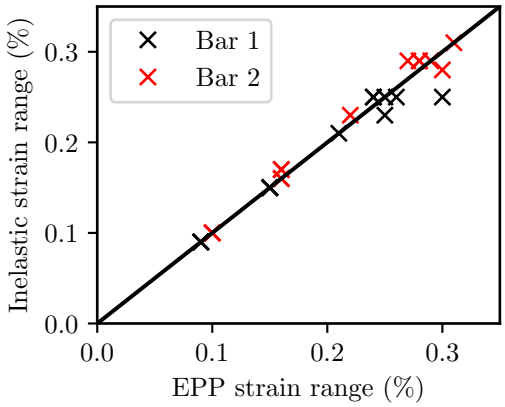

Figure 2.5: Graphical summary of the data in Table 2.1.

a nozzle leading to a pipe. The vessel head thickness is 1 inch, the vessel radius is 26.5 inches, the pipe thickness is 0.5 inches, and the pipe outer radius is 3 inches. The vessel, nozzle, and pipe is subject to a cyclic pressure, shown in the figure, and a cyclic imposed displacement on the pipe represents a load from a piping system. The whole structure is held at $T = 650^\circ$ C.

The results in Fig. 2.7 compare a full inelastic analysis to a consistent EPP design analysis. Both simulations repeat the load cycle 20 times and compare the ASME Section III, Division 5 equivalent strain range, plotted over the critical nozzle region. The EPP strains well represent the full inelastic strain distribution, matching the location and relative magnitude of the critical, highest strain range. Discrepancies between the EPP and the full inelastic strains tend to be conservative, i.e. the EPP strain range exceeds the full inelastic strain range. Overall this example shows that the EPP method can reliably bound strain ranges in realistic high temperature components under realistic loads. Taken together, these validation examples demonstrate the EPP method is a suitable analysis method for determining design strain ranges for use with the improved creep-fatigue design method.

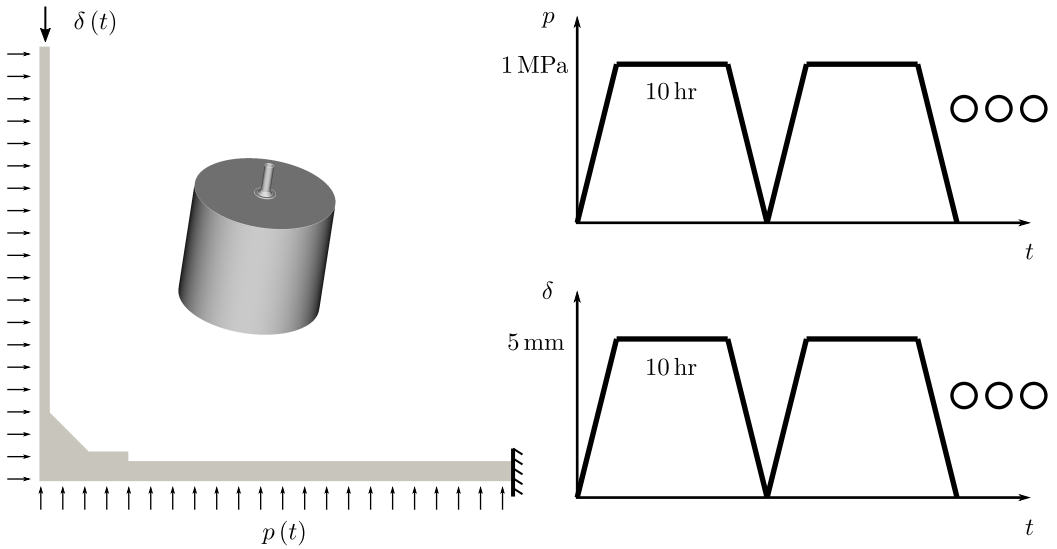

Figure 2.6: Axisymmetric simulation of a nozzle subject to a cyclic pressure and piping load

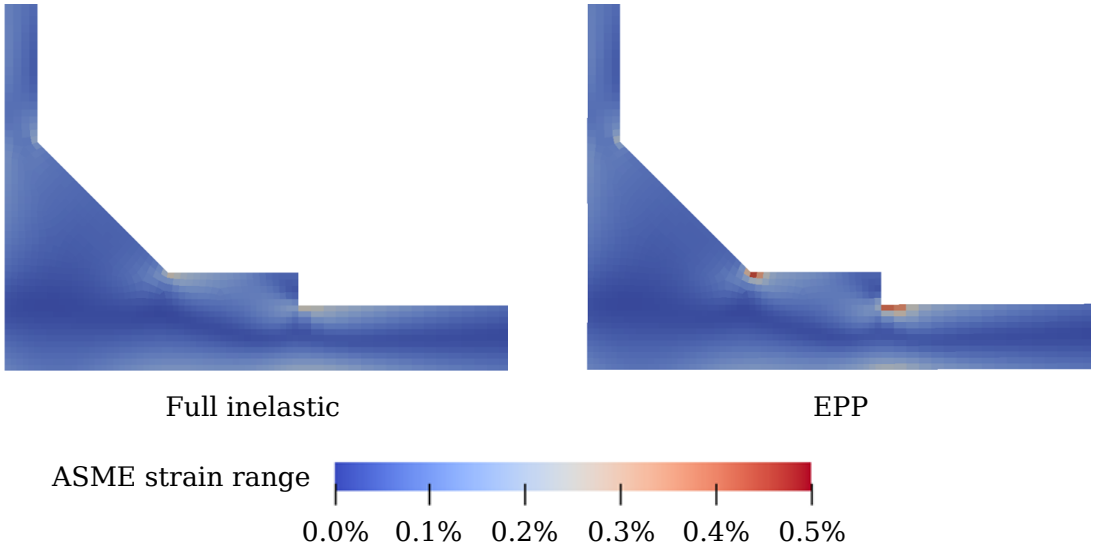

Figure 2.7: Fringe plot comparing a full inelastic simulation to a consistent EPP simulation of the nozzle problem defined in Fig. 2.6.

3 Progress on SMT design curves

The focus of this report is on developing the EPP method for representing design strain ranges in components in high-temperature reactor operating conditions. This chapter provides a brief overview of the challenges in developing the second part of the complete design method, the creep-fatigue design curves.

These curves will be developed from a database of experiments on SMT specimens. In these tests the strain range, hold time, follow up factor, and temperature can all be controlled independently. However, the design lives of actual reactor structural components will far exceed the times examined directly in the experiments. Methods will be required to extrapolate shorter hold times to longer hold times and to extrapolate larger strain ranges to smaller strain ranges that cause failure in a longer amounts of time.

Previous work at Oak Ridge National Laboratory has collected data for several materials using Type 1 and Type 2 SMT specimens, along with pressurized SMT tests [10–12]. This data covers a wide range of temperatures, hold times, and elastic follow up factors. Of all the test temperatures and test materials the most data is currently available for Alloy 617 at 950° C. Figure 3.1 plots the available data for this material at this temperature in the form that will be used for the design charts: a plot of strain range versus number of cycles to failure.

Qualitatively, the data matches the expected trends. Creep-fatigue loading is more damaging than pure fatigue loading and creep-fatigue loading with higher follow up is more damaging than simple creep-fatigue loading with a follow up factor of $q = 1$. The green circle on the plot is a Type 1 SMT specimen under pure fatigue loading, which is why it has a higher than expected number of cycles to failure.

Given data of this type the steps towards creating a design curve would be:

1. Develop a model that explains and can extrapolate the data. This model should have the form
$$N_f = F\left(\Delta\varepsilon, t_h, q, T\right)$$
where N_f is the number of cycles to failure, $\Delta\varepsilon$ is the strain range, t_h the hold time, q the follow up factor, and T the temperature.

2. From engineering judgement and analysis of representative structural components determine bounding values for the elastic follow up factor q and the hold time t_h. This reduces the model to a series of temperature dependent curves plotting the strain range versus the number of cycles to failure. These would be the design curves for the new creep-fatigue method.

3. Thus far the model would apply only to uniaxial load. The final step is to develop a definition of the scalar equivalent strain range to capture observed multiaxial stress state dependence in the failure data.

The previously collected data in Fig. 3.1 and similar data at other temperatures and for other materials can be used to begin to work on a model. However, there is a significant challenge in using the previous Type 1 and Type 2 SMT test data. These specimens did not all fail in the straight gauge region of the specimens. Instead, many failed near the transition radius stepping between the outer and inner diameters. The stress state near

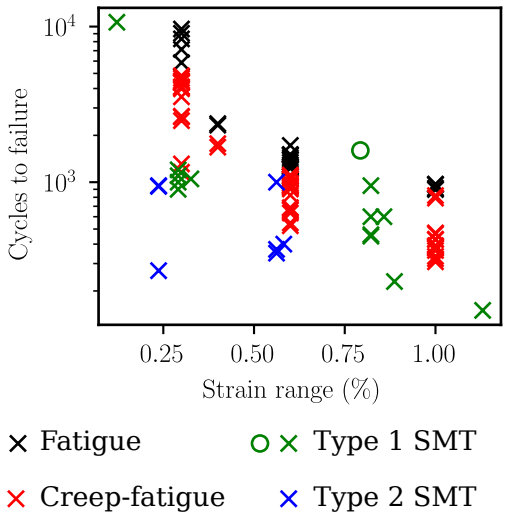

Figure 3.1: Available experimental data for Alloy 617 at 950° C.

this transition is not uniaxial, which complicates interpreting the failure data from these experiments. Oak Ridge National Laboratory is developing test procedures which enforce a uniaxial stress state at the failure location in SMT tests, still including follow up effects. These tests are described in a companion report issued by ORNL [13]. Data from these tests will be used, going forward, to develop the design curves following the process outlined above.

The previous Type 1 and Type 2 sample data is still useful. It can be used to validate the overall design procedure, including the equivalent strain range capturing multiaxial stress state effects. A successful final design method should be able to predict the location of failure (center gauge or near transition) in the previous SMT tests as well as bound the measured number of cycles to failure. In addition, the specimens that failed in the straight gauge portion of the test article can be included in the uniaxial database of result used to determine the design curves.

4 Conclusions

4.1 Summary

This report develops a design analysis method for the cyclic stable strain range in structural components in high temperature service. The method is based on an elastic perfectly plastic (EPP) analysis using a pseudoyield stress selected from values of the material isochronous stress-strain curves. Several validation examples demonstrate the effectiveness of the method in representing strain ranges in simple experimental tests and more complex, realistic structural components.

4.2 Future work

For the strain range analysis method future work should concentrate on providing a rigorous proof of the proposed bounding method and on additional validation examples, likely focusing on consistent comparisons to full inelastic simulations. Both efforts would support the use of the EPP method in the design of high temperature nuclear structural components.

One additional issue to address will be the applicability of the proposed method of bounding strain ranges to cyclic softening materials. These types of materials may not have the stability required in the Frederick and Armstrong proof that the material response will become steady. As such, modifications to the method may be needed to account for softening.

Chapter 3 provides an outline describing how to develop design curves from SMT data. That chapter noted the challenges in using the existing Type 1 and Type 2 SMT test data to formulate design curves but also noted that Oak Ridge National Laboratory has recently developed improved test protocols that ensure future data will be collected for uniaxial failures. Additionally, the improved test procedure provides finer control of the follow up factor q, which could aid the development of a model to represent the test failure data by providing finer granularity in the data for that particular test variable. With some caution, inelastic modeling can also be used to develop methods for extrapolating creep-fatigue type test data with follow up effects by directly simulating the new SMT test configurations. These simulations would need to include a damage model to represent creep-fatigue failure. This damage model would need to be selected carefully, in order to model realistic creep-fatigue failure.

The final issue to be addressed is defining an effective strain measure to accurately represent multiaxial failure. Chapter 3 noted that the Type 1 and Type 2 SMT data could be valuable for validating this strain measure. However, the stress state near the transition in the SMT specimens is complicated. Creep-fatigue failure data, with follow up effects, for simple test specimens with an easily-defined stress state would be more valuable for developing the procedure to account for multiaxiality. Future work, in collaboration with ORNL, will develop tests of this type.

Acknowledgments

The research was sponsored by the U.S. Department of Energy (DOE), under Contract No. DE-AC02-06CH11357 with Argonne National Laboratory, managed and operated by UChicago Argonne LLC. Programmatic direction was provided by the Office of Advanced Reactor Technologies (ART) of the Office of Nuclear Energy (NE).

The authors gratefully acknowledge the support provided by Alice Caponiti, Director, Office of Advanced Reactor Technologies (ART), Sue Lesica, Federal Manager, ART Advanced Materials Program, and Hans Gougar of INL, National Technical Director, ART Gas-Cooled Reactors Campaign.

Bibliography

[1] American Society of Mechanical Engineers. Case N-861: Satisfaction of Strain Limits for Division 5 Class A Components at Elevated Temperature Service Using Elastic-Perfectly Plastic Analysis. In *ASME Boiler and Pressure Vessel Code, Nuclear Component Code Cases*. 2015.

[2] American Society of Mechanical Engineers. Case N-862: Calculation of Creep-Fatigue for Division 5 Class A Components at Elevated Temperature Service Using Elastic-Perfectly Plastic Analysis. In *ASME Boiler and Pressure Vessel Code, Nuclear Component Code Cases*. 2015.

[3] American Society of Mechanical Engineers. Section III, Division 5. In *ASME Boiler and Pressure Vessel Code*. 2017.

[4] J Bree. Elastic-plastic behaviour of thin tubes subjected to internal pressure and intermittent high-heat fluxes with application to fast-nuclear-reactor fuel elements. *The Journal of Strain Analysis for Engineering Design*, 2(3):226–238, 1967.

[5] P. Carter. Bounding theorems for creep-plasticity. *International Journal of Solids and Structures*, 21(6):527–543, 1985.

[6] Peter Carter. Analysis of cyclic creep and rupture. Part 1: Bounding theorems and cyclic reference stresses. *International Journal of Pressure Vessels and Piping*, 82(1): 15–26, 2005.

[7] Peter Carter. Analysis of cyclic creep and rupture. Part 2: Calculation of cyclic reference stresses and ratcheting interaction diagrams. *International Journal of Pressure Vessels and Piping*, 82(1):27–33, 2005.

[8] Peter Carter, Robert I. Jetter, and T.-L. Sham. Application of elastic-perfectly plastic cyclic analysis to assessment of creep strain. In *Proceedings of the ASME 2012 Pressure Vessels & Piping Division Conference*, 2012.

[9] C. O. Frederick and P. J. Armstrong. Convergent internal stresses and steady cyclic states of stress. *The Journal of Strain Analysis for Engineering Design*, 1(2):154–159, 1966.

[10] T.-L. Sham, Robert I Jetter, and Yanli Wang. Elevated temperature cyclic service evaluation based on elastic-perfectly plastic analysis and integrated creep-fatigue damage. In *Proceedings of the ASME 2016 Pressure Vessels and Piping Conference*, pages 1–10, 2016.

[11] Yanli Wang, Robert I Jetter, Kapil Krishnan, and T.-L. Sham. Progress Report on Creep-Fatigue Design Method Development Based on SMT Approach for Alloy 617. Technical report, 2013.

[12] Yanli Wang, T-L Sham, and Robert I Jetter. Alloy 617 Creep-Fatigue Damage Evaluation Using Specimens With Strain Redistribution. *Journal of Pressure Vessel Technology*, 137(2):21402, 2015.

[13] Yanli Wang, Robert I. Jetter, Mark C. Messner, and T.-L. Sham. Report on FY18 Testing Results in Support of Integrated EPP-SMT Design Methods Development. Technical Report ORNL/TM-2018/887, Oak Ridge National Laboratory, 2018.

Distribution List

Name	*Affiliation*	*Email*
Caponiti, A.	DOE	alice.caponiti@nuclear.energy.gov
Croson, D.	INL	diane.croson@inl.gov
Gouger, H. D.	INL	hans.gougar@inl.gov
Hill, R. N.	ANL	bobhill@anl.gov
Krumdick, G. K.	ANL	gkrumdick@anl.gov
Lesica, S.	DOE	sue.lesica@nuclear.energy.gov
Li, D.	DOE	diana.li@nuclear.energy.gov
McMurtrey, M.	INL	michael.mcmurtrey@inl.gov
Messner, M. C.	ANL	messner@anl.gov
Qualls, A. L.	ORNL	quallsal@ornl.gov
Sham, T.-L.	ANL	ssham@anl.gov
Singh, D.	ANL	dsingh@anl.gov
Travis, T. R.	INL	travis.mitchell@inl.gov
Wang, Y.	ORNL	wangy2@ornl.gov
Wright, R.	INL	richard.wright@inl.gov
Zhang, X.	ANL	xuanzhang@anl.gov

Applied Materials Division
Argonne National Laboratory
9700 South Cass Avenue, Bldg. 208
Argonne, IL 60439

www.anl.gov